SUPPLEMENTARY INFORMATION

STAT3 promotes corticospinal remodeling and functional recovery after spinal cord injury

Claudia Lang[1], Peter M. Bradley[1], Anne Jacobi[1], Martin Kerschensteiner[1,2]* and Florence M. Bareyre[1,2]*

[1] Institute of Clinical Neuroimmunology, Ludwig-Maximilians Universität, Munich, Germany

[2] Munich Cluster for Systems Neurology (SyNergy), Munich, Germany

* equal contribution

SUPPLEMENTARY METHODS

Generation and production of AAV vectors

rAAV-STAT3 and Control rAAV were cloned and produced as previously described [1,2]. Briefly, for engineering pAAV-STAT3, the STAT3 gene was excised from pcDNA3 STAT3 (Addgene plasmid 8706) with BamHI and XhoI and cloned into the pAAV-MCS vector (Stratagene) at the HincII site. Control pAAV-ECFP was engineered by excising the ECFP gene from the pECFP N1 plasmid at BamHI and NotI and then it was cloned into the pAAV-MCS at the HincII site. Control pAAV-mbEYFP was constructed by excising the EYFP gene from an engineered pmbEYFP N1 plasmid at XhoI and NotI and then it was cloned into the pAAV-MCS at the BmgBI site.

Genomic titers were as follows: rAAV-STAT3, 9×10^{12} genome copies/ml; Control rAAV-ECFP, 9.2×10^{12} genome copies/ml; Control rAAV-mbEYFP, 1.7×10^{11} genome copies/ml. One microliter of undiluted rAAV solution was injected in all experiments.

Surgical procedures

Midthoracic hemisection, labeling of the hindlimb CST (hCST) fibers and long propriospinal neurons: Mice were anesthetized with a subcutaneous injection of ketamin/xylazine (ketamine 100 mg/kg, xylazine 13 mg/kg). After a laminectomy at thoracic level 8 (T8), a midthoracic dorsal hemisection, which results in a transection of the main dorsal and minor dorso-lateral CST component, was performed with fine iridectomy scissors. The lesion extent was assessed on spinal cord cross sections spanning the thoracic lesion site. Following staining with a fluorescent Nissl dye (NT435, dilution 1:500) the sections were scanned using an Olympus FV1000 confocal microscope. Image stacks were then processed with ImageJ and the lesion area, including both the cavity and surrounding damaged tissue, was outlined. To quantify the lesion volume, the measured lesion area of each section was multiplied by the section

thickness (50μm) and the results of consecutive sections spanning the entire lesion extension were summed up for each animal to provide a final estimation of the total lesion volume. Prior to and after surgery animals were administered Meloxicam (Metacam, Boehringer Ingelheim) once per day for 2 days. One week prior to the lesion, 1μl of rAAV-STAT3 or control rAAV-ECFP was pressure-injected into the hindlimb motor cortex using a finely pulled glass micropipette (coordinates from bregma: -1.0mm caudal; 0.8mm lateral; 0.6mm depth). The hindlimb CST was traced using 1μl of a 10% (in 0.1M PB) solution of biotinylated dextran amine (BDA, 10 000 MW, Life technologies) two weeks prior to sacrifice date using the coordinates: −1.3 mm posterior to bregma, 1 mm lateral to bregma, 0.6mm depth as previously described [3]. Long propriospinal neurons were then retrogradely traced by pressure injections of 1μl of 10% fluoroemerald (dextran, fluorescein, 10 000 MW, Life technologies) into each side of the spinal cord at thoracic level 12 as previously described for rats [4]. Mice were sacrificed 1, 3 or 12 weeks after dorsal hemisection.

Pyramidotomy, labeling of the forelimb CST fibers, short propriospinal neurons and motoneurons: A unilateral lesion of the CST at the level of the pyramidal decussation was performed using a ventral approach as previously described for rats [5]. Briefly, the left medullary pyramid was exposed through an opening of the occipital bone. A unilateral lesion of the left CST rostral to the decussation was made with a fine (tungsten) metal wire using the basilar artery as a landmark for the midline. The extent of the lesion was verified in all cases by histological analysis of the lesion site in Nissl-stained tissue sections. Mice were left to recover on a warming blanket until they regained consciousness. Prior to and after surgery animals were administered meloxicam (Metacam, Boehringer Ingelheim) once per day for 2 days. One week prior to the lesion, 1μl of rAAV-STAT3 or rAAV-mbYFP was injected into the right forelimb motor cortex using a fine pulled glass micropipette (coordinates from

bregma: -0.6mm caudal, 1mm lateral, 0.7mm depth). One µl of a 10% (in 0.1M PB) solution of biotinylated dextran amine (BDA, 10 000 MW, Life technologies) was used to trace the right intact CST one week prior to sacrifice date (coordinates from bregma: -0.6mm caudal, 1mm lateral, 0.7mm depth). Short propriospinal neurons were then retrogradely traced by pressure injections of 1µl fluoroemerald into each side of the spinal cord at thoracic level 1/2 as previously described [4]. Motoneurons were retrogradely labeled from the forelimb muscles using 1µl Cholera Toxin Alexa Fluor 647 (Life technologies) injected with a Hamilton syringe. Mice were sacrificed 1, 3 or 12 weeks after pyramidotomy.

Tissue processing and histological analysis

Brains and spinal cords were dissected and postfixed overnight in PFA. The tissue was then cryoprotected in 30% sucrose (Sigma) for 3 days. Coronal sections (50µm thick) were cut on a cryostat. To visualize CST collaterals, BDA detection was performed as follows: Sections were incubated in ABC complex (Vector Laboratories) overnight at 4°C. After a 20 min tyramide amplication (Biotin-XX, TSA Kit #21, Life technologies) sections were incubated overnight with Streptravidin conjugated to Alexa Fluor 594 (1:500, Life technologies). For STAT3 immunohistochemistry, antigen retrieval with Tris-EDTA was performed prior to immunostaining. After blocking for 1 hour, an anti-STAT3 antibody (dilution 1:500; Cell Signaling) or anti p-STAT3 antibody (dilution 1:50; Cell Signaling) diluted in PBS containing 0.1% Triton X-100 (Sigma) and 2.5% goat serum serum (Life technologies) was added. Sections were then incubated at 4°C overnight. The following day, the appropriate secondary antibodies (goat anti rabbit antibodies conjugated with Alexa Fluor 594 or Alexa Fluor 488) were applied. Counterstaining was performed using NeuroTrace 435 (Invitrogen) and sections were mounted in Vectashield (Vector Laboratories). The percentage of p-STAT3 positive neurons was determined by counting the number of NeuroTrace positive neurons and the number of neurons that were p-STAT3 positive in layer V of ten consecutive sections (50µm

thick) surrounding the injection site (five before and five after the injection site; imaging field of 423µm x 423µm). A ratio was made by dividing the number of p-STAT3 positive neurons by the total number of NeuroTrace positive neurons in the imaging field. For the retrograde labeling of CST projection neurons, animals were injected with rAAV-STAT3 one week prior to the injury. Immediately following the midthoracic dorsal hemisection, 2µl of a retrograde tracer (dextran tetramethylrhodamine 3 000 MW, 10% in 0.1M PB, Life technologies) was injected into the spinal cord at the site of injury (0.3mm lateral from the midline, 0.3mm depth) using a finely pulled glass micropipette. Three weeks following lesion (and injection of dextran tetramethylrhodamine), mice were sacrificed and then processed as described above. Consecutive 50µm thick cross-sections of the motor cortex (-0.96 to -1.26mm from bregma, covering the entire area that contained retrogradely labeled neurons) were evaluated by two independent observers and averaged to determine the percentage of retrogradely-labelled neurons that express p-STAT3.

To assess the density of neurons, the motor cortex of *Emx*-Cre x $STAT3^{fl/fl}$ mice and their Cre negative littermates (perfused 3 weeks post spinal cord injury) were processed and stained overnight with an antibody against NeuN (dilution 1:500). Consecutive sections were evaluated and the density of NeuN positive neurons in Layer V of the motor cortex was quantified.

Quantification of CST growth

To determine the effect of sustained STAT3 expression or STAT3 deletion on the growth of CST fibers after a midthoracic dorsal hemisection, we analyzed consecutive longitudinal sections of the midthoracic spinal cord. Image stacks were recorded on an Olympus FV1000 confocal microscope with a x20/0.85 oil immersion objective. The number of BDA-labeled growing fibers in the dorsal funiculus that intersected with a dorso-ventral lines positioned every 100µm distal from the lesion site was counted. The lesion site was

identified visually and level 0 was positioned at the end of the retracting non growing fibers. The total number of growing fibers counted on 4-5 consecutive longitudinal 50μm thick sections was then normalized to the number of fibers in the main CST tract (obtained from the dorsal funiculus at cervical C5 level) and divided by the number of sections evaluated. The value obtained for a given distance is the number of CST fibers per labeled CST axons per section, the "fiber number index" [6]. To exclude a contribution from spared fibers, only fibers emerging from the dorsal main CST and extending in the dorsal funiculus were counted. To confirm that all dorsal main CST axons were cut by the lesion, we verified the absence of labeled dorsal fibers further distal from the site of the lesion (at thoracic level 11) in all animals used for the analysis of the effects of sustained STAT3 activation on axon growth (n=14 mice). To quantify axonal sprouting, we counted the number of collateral sprouts emerging from the transected axons and normalized this number to the number of traced CST fibers. All quantifications were performed by an observer blinded with respect to injury status and treatment.

Quantification of CST remodeling

To evaluate axonal remodeling following a midthoracic dorsal hemisection, traced CST collaterals entering the grey matter at cervical levels C4 were counted on 30 consecutive coronal sections per animal using a light microscope (Olympus IX471) with a x40/0.65 air objective. To correct for differences in inter-animal tracing efficiency, the number of collaterals was divided by the number of traced fibers in the main CST tract and expressed as the ratio of collaterals per main CST fiber [4]. To evaluate axonal remodeling following a unilateral pyramidotomy, we counted traced CST fibers crossing the midline on 30 sections per animal using a light microscope. Again numbers were normalized to the number of traced fibers in the main CST tract and expressed as the ratio of midline crossing fibers per main CST fiber [5]. To assess the projection pattern of these midline crossing CST fibers in the

denervated side of the spinal cord, we counted the number of CST collaterals invading laminae I to V and VI to IX of the spinal cord and related to the total number of fibers crossing the midline. To assess the extension of fibers into the denervated side, we counted the number of CST collaterals crossing lines spaced in 25µm intervals from the midline into the gray matter of the denervated side of the cord. Values obtained were normalized to the number of fibers in the main CST tract and expressed as the density of midline crossing fibers. All quantifications were performed by an observer blinded with respect to injury status and treatment.

Behavioral analysis

BMS: We used the Basso mouse scale [7] to assess recovery of hindlimb locomotion after a spinal lesion. Following the ranking system previously described [7] mice were given scores from 0-9, with a score of 0 indicating no ankle movement and a score of 9 indicating frequent or consistent plantar stepping, mostly coordinated stepping, paws parallel at initial contact and lift off, normal trunk stability and tail consistently up. For evaluation, the mice were placed in an open field for 4 min and assessed by two observers blinded to the genotype of the mice. Mice were assessed before and 2, 7, 14 and 21 days after lesion.

Rotarod: To assess balance, coordination and motor control after injury, mice were tested using the Rotarod performance test [8]. Prior to injury mice were habituated to the apparatus every 3 days over a 2 week period. For testing, mice are placed in one of the four lanes that have a motor driven rod. The system records the velocity of the rod and the time at which the mouse falls from the rod onto the beam below. The performance of the mice was evaluated using two different paradigms: rotarod rotation at a fixed speed (20 rpm) and accelerating rotarod rotations (4-40 rpm). For accelerating rotarod rotations, the speed of the rotation and latency up to the fall were recorded. For each mouse the best performance after

three trials (with 15min intervals) was used. Rotarod performance was assessed before and 2, 7, 14 and 21 days after injury.

Food pellet grasping: To assess the recovery of forelimb function after pyramidotomy we used the food pellet staircase reaching test as previously described [9,10]. Mice were first accustomed to retrieve sucrose pellets (Bio-Serv) from a baited double staircase (Campden Instruments) two weeks before baseline recordings were taken. After unilateral pyramidotomy, mice were then tested starting at 2 days post-lesion and then weekly for up to 10 weeks after lesion. Prior to testing, mice were food deprived for 12 hours. Sessions lasted 15 min and the number of pellets eaten, displaced as well as the lowest step at which no pellet remained was recorded. For re-lesion experiments the contra-lateral (unlesioned) CST of mice treated with rAAV-STAT3 was cut on the level of the pyramids at 10 weeks after the initial pyramidotomy and the mice were tested 3 days after the contralateral pyramidotomy (n = 13 mice).

Electrophysiology

Determination of optimal coordinates for stimulation of forelimb motor cortex: From preliminary mapping experiments we determined the spatial centre of the motor cortex region that controlled forelimb movements to be around +0.4mm from bregma and 1.2mm lateral from the midline, which is consistent with previous studies [4,11]. We observed that forelimb responses to cortical stimulation were strongest in the more posterior areas of the forelimb region, corresponding to the region -0.2 to +0.1mm from bregma. In addition, we also obtained the greatest amount of forelimb-projecting CST labeling when tracers or viruses were introduced in this area. Therefore we injected rAAV expressing either membraneYFP or STAT3 at -0.4mm from bregma, 1mm lateral, and 0.6mm depth, corresponding to cortical layer V of the caudal border of the forelimb region. We injected the viruses slightly caudal of

the target region as we previously observed that diffusion of injected viruses or tracers into motor cortex is biased in the anterior direction.

Electrophysiological recordings: Animals were anaesthetized with an intraperitoneal injection of ketamine/xylazine (ketamine, 100mg/kg; xylazine, 13 mg/kg), and then supplemented with subdermal injections of ketamine alone (33mg/kg) as needed by assessment of the breathing rate and hindpaw pinch response. A craniotomy was made that extended approximately 0.8mm anterior to 0.8mm posterior from bregma and from 0.5 to 1.5mm lateral of midline, over the sensorimotor cortex of the right hemisphere. The dura was removed and the exposed brain was kept moist with saline. Unipolar stimulation of the right motor cortex was performed using parylene insulated tungsten microelectrodes of 1MΩ impedance (TM33B10, WPI). A chlorinated silver wire was placed in contact with the brain at the anterior-lateral edge of the craniotomy and served as the return electrode. Differential EMG recording in the ipsilateral forelimb was performed using hook electrodes in bipolar configuration, made from 50µm Teflon-coated steel wire (A-M Systems Inc.), with the tips of the hooks exposed. The electrodes were inserted into the forelimb flexor muscle group using a 25-gauge needle which was then withdrawn. The forelimbs were then placed in an elevated position on foam pads to assist visualization of muscle movements and to maintain correct placement of the hook electrodes. Signals were amplified (5k), band-pass filtered (low 300Hz, high 3kHz, NPI electronics, Tamm) and digitized using a Micro 1401 data acquisition unit (CED Ltd; Cambridge Electronic Design, UK) and sent to a computer running Spike2 software (Cambridge Electronic Design, UK).

Stimulation protocol: Stimulations were performed at four sites in the anterior-posterior direction along the middle of the forelimb motor cortex region, starting at the centre of the region (+0.4mm from bregma, 1.2mm lateral) and then at three further evenly spaced

sites back to the rostral edge of the scar that had formed at the virus injection site (-0.2mm from bregma, 1.2mm lateral). If necessary, slight adjustments in the mediolateral direction were made to prevent the electrode from penetrating blood vessels. Monophasic cathodal pulses (10ms train duration at 300Hz, 0.2ms pulse duration) were applied through the electrode at an interval of 1s using an iso-flex stimulus isolator triggered by a Master 8 stimulator (both from A.M.P.I. Instruments). The electrode was lowered vertically into the cortex initially using a high stimulus current (60-90μA) until movement of the contralateral forelimb was detected (20 trials per site). Forelimb activation was classified as a movement of the digits, the distal or proximal joints and/or muscle twitch. To determine the threshold of ipsilateral forelimb activation, the depth of the electrode was first optimized to give maximal contralateral forelimb movement. At this point the current was reduced to zero, and then increased in increments of 10μA until EMG signal in the ipsilateral forelimb appeared. If no EMG signal was detected at 250μA the site was deemed unresponsive. In situations where no response was evident, it was confirmed that the hook electrodes were correctly positioned and functional by squeezing the ipsilateral paw. It should be noted that using our stimulation protocol ipsilateral forelimb responses were detected in all unlesioned animals (n=7 mice; average threshold 49.5μA, average latency 0.0137s) an observation which has been extensively documented by others [12-14]. These ipsilateral responses are likely due to inter-hemispheric connections that cross the midline above the level of the medulla oblongata and are thus removed by the initial pyramidotomy [14]. Latencies were also determined and measured to the onset of the EMG response. Further we averaged EMG traces (generally 10 cycles or more) and measured the duration and amplitude of the peak-to-peak response in unlesioned control mice (average duration=0.0163±0.0031s, average amplitude=0.1226±0.0549mV, n=6 mice) as well as in lesioned mice at 12 weeks after injection with Control rAAV (average duration=0.0068±0.0007s, average

amplitude=0.0439±0.0059mV, n=8 mice) or rAAV-STAT3 (average duration=0.0101±0.0013s, average amplitude=0.1020±0.051mV, n=8 mice).

Statistical evaluation

Data were analyzed by the Student's t test in case of comparisons of two groups and one-way ANOVA with Tukey test or two-way ANOVA with Bonferroni test in case of multiple comparisons using Graphpad Prism 5.01 for Windows (GraphPad Software).

SUPPLEMENTARY REFERENCES

[1] Klugmann M, Symes CW, Leichtlein CB, Klaussner BK, Dunning J, Fong D, Young D, During MJ (2005) AAV-mediated hippocampal expression of short and long Homer 1 proteins differentially affect cognition and seizure activity in adult rats. *Mol Cell Neurosci.* **28**: 347–60

[2] Bareyre FM, Garzorz N, Lang C, Misgeld T, Büning H, Kerschensteiner M (2011) In vivo imaging reveals a phase-specific role of STAT3 during central and peripheral nervous system axon regeneration. *PNAS* **108**: 6282-7

[3] Lang C, Guo X, Kerschensteiner M, Bareyre FM (2012) Single collateral reconstructions reveal distinct phases of corticospinal remodeling after spinal cord injury. *PLoS ONE* **7**: e30461

[4] Bareyre FM, Kerschensteiner M, Raineteau O, Mettenleiter TC, Weinmann O, Schwab ME (2004) The injured spinal cord spontaneously forms a new intraspinal circuit in adult rats. *Nat Neurosci* **7**: 269-77

[5] Bareyre FM, Haudenschild B, Schwab ME (2002) Long-Lasting Sprouting and Gene Expression Changes Induced by the Monoclonal Antibody IN-1 in the Adult Spinal Cord. *J Neurosci* **22**: 7097-110

[6] Liu K *et al* (2010) PTEN deletion enhances the regenerative ability of adult corticospinal neurons. *Nat Neurosci* **13**: 1075-81

[7] Basso D, Fisher L, Anderson A, Jakeman L, McTigue D, Popovich P (2006) Basso Mouse Scale for locomotion detects differences in recovery after spinal cord injury in five common mouse strains. *J Neurotrauma* **23**: 635-59

[8] McGavern DB, Zoecklein L, Drescher KM, Rodriguez M (1999) Quantitative Assessment of neurologic deficits in a chronic progressive murine model of CNS demyelination. *Exp Neurol* **158**: 171-181

[9] Baird AL, Meldrum A, Dunnett SB (2001) The staircase test of skilled reaching in mice. *Brain Res Bull* **54**: 243-50

[10] Starkey ML, Barritt AW, Yip PK, Davies M, Hamers FPT, McMahon SB, Bradbury EJ (2005) Assessing behavioural function following a pyramidotomy lesion of the corticospinal tract in adult mice. *Exp Neurol* **195**: 524-539

[11] Tennant KA, Adkins DL, Donlan NA, Asay AL, Thomas N, Klein JA, Jones TA (2011) The organization of the forelimb representation of the C57BL/6 mouse motor cortex as defined by intracortical microstimulation and cytoarchitecture. *Cereb Cortex* **21**: 865-76

[12] Kartje-Tillotson G, Neafsey EJ, Castro AJ (1985) Electrophysiological analysis of motor cortical plasticity after cortical lesions in newborn rats. *Brain Res* **332**: 103-11

[13] Z'Graggen WJ, Fouad K, Raineteau O, Metz GA, Schwab ME, Kartje, GL (2000) Compensatory sprouting and impulse rerouting after unilateral pyramidal tract lesion in neonatal rats. *J Neurosci* **20**: 6561-9

[14] Brus-Ramer M, Carmel JB, Martin JH (2009) Motor cortex bilateral motor representation depends on subcortical and interhemispheric interactions. *J Neurosci* **29**: 6196-206

SUPPLEMENTARY FIGURES

Supplementary Figure S1: STAT3 expression in cortical neurons is transiently induced after spinal cord injury and can be conditionally deleted

(**A**,**B**) Confocal images illustrating the expression of STAT3 in layer V cortical neurons (green, NeuroTrace 435; red, STAT3) of an unlesioned mouse (**A**) or a mouse perfused 24hrs following a midthoracic hemisection (**B**). (**C**) Quantification of STAT3 expression in layer V cortical neurons in unlesioned mice (white bar) and mice perfused at different timepoints following a midthoracic hemisection (grey bars, n=4-6 mice per group). (**D**,**E**) Confocal images illustrating the expression of STAT3 in layer V cortical neurons (green, NeuroTrace 435; red, STAT3) in STAT3 competent (**D**) and conditional STAT3 deficient mice (**E**) perfused 3wks following a midthoracic hemisection. **(F**) Quantification of STAT3 expression in layer V cortical neurons of unlesioned mice (white bar, same as in **C**), STAT3 competent (grey bar) and conditional STAT3 deficient mice (blue bar) perfused 3wks following a midthoracic hemisection (n=5 mice per group). All bars and error bars in this figure represent mean±SEM. Statistical analysis was performed using a one-way ANOVA followed by Tukey test. *, $P<0.05$; **, $P<0.01$. Scale bars equal 50μm in **B** (also for **A**) and 100μm in **E** (also for **D**).

Supplementary Figure S2: Conditional deletion of STAT3 does not affect neuronal cell density in layer V of the motor cortex

(**A-D**) Confocal images of the motor cortex of STAT3 competent and STAT3 deficient mice that were immunostained with an anti NeuN antibody. (**E**) Quantification of the number of NeuN positive neurons in layer V of the motor cortex of STAT3 competent (grey bar) and STAT3 deficient (blue bar) mice (n=5 mice per group). All bars and error bars in this figure

represent mean±SEM. Statistical analysis was performed using a t-test. Scale bar equals 100 µm in **B** (also for **A**) and **D** (also for **C**).

Supplementary Figure S3: Conditional deletion of STAT3 does not affect CST growth early after spinal cord injury

(**A**) Schematic representation of the analysis of CST growth at the lesion site following spinal cord injury. (**B**,**C**) Quantification of the sprouting (**B**) and growth (**C**) of lesioned CST fibers in STAT3 competent (grey bars, n=5) and conditional STAT3 deficient mice (blue bars, n=5) at 1 wk after lesion. (**D**,**E**) Confocal images of longitudinal sections of the spinal cord (lesion indicated by asterisk) illustrating growth of the corticospinal tract (in red) in STAT3 competent mice (**D**) and conditional STAT3 deficient mice (**E**). The dotted lines in (**D**) represent the distances at which the growing axons were counted. (**F**) Schematic representation of the analysis of CST remodeling following spinal cord injury. (**G**,**H**) Confocal images of cervical hindlimb CST collaterals in lesioned STAT3 competent (**G**) and conditional STAT3 deficient (**H**) mice 1 wk following spinal cord injury. (**I**) Quantification of the number of collaterals exiting the hindlimb CST tract in the cervical spinal cord in STAT3 competent (grey bar, n=8) and conditional STAT3 deficient mice (blue bar, n=8) 1 wk following spinal cord injury. All bars and error bars in this figure represent mean±SEM. Statistical analysis was performed using a repeated one-way ANOVA followed by Tukey test in **C** and a t-test in **B**, **I**. Scale bars equal 100µm in **E** (also for **D**) and 50 µm in **H** (also for **G**).

Supplementary Figure S4: Conditional deletion of STAT3 in cortical projection neurons does not influence functional recovery following spinal cord injury

(**A**) Quantification of the BMS score before and up to 3 weeks following spinal cord injury in STAT3 competent (grey bars) and conditional STAT3 deficient (blue bars) mice (n=10-17 mice per group). (**B**) Quantification of the endurance time at a fixed rotorod speed before and up to 3 weeks following spinal cord injury in STAT3 competent (grey squares) and conditional STAT3 deficient (blue squares) mice (n=10-17 mice per group). (**C**) Quantification of the endurance time at an accelerated rotorod speed before and up to 3 weeks following spinal cord injury in STAT3 competent (grey squares) and conditional STAT3 deficient (blue squares) mice (n=10-17 mice per group). All bars and error bars in this figure represent mean±SEM. Statistical analysis were performed using a repeated one-way ANOVA followed by Tukey test. ***, P<0.001.

Supplementary Figure S5: Sustained expression of STAT3 increases growth of CST axons at the lesion site

(**A**) Schematic representation of the analysis of CST growth at the lesion site following spinal cord injury. (**B-E**) Confocal images of longitudinal sections of the spinal cord (asterisk, indicates lesion site) illustrating growth of the transected CST axons (BDA, white) in mice injected with rAAV-STAT3 (**B-D**) or Control rAAV (**E**). The dotted lines in (**E**) represent the distances at which growing CST axons were counted. Boxed areas in (**B**) are magnified 2-times in (**C**) and (**D**). (**F**,**G**) Quantification of axonal growth at different distances distal from the lesion site (**F**) and of axonal sprouting (**G**) at the site of the lesion in mice injected with Control rAAV (grey bars) and mice injected with rAAV-STAT3 (red bars) perfused 3 wks following midthoracic hemisection (n=7 mice per group). All bars and error bars in this figure represent mean±SEM. Statistical analysis was performed using a repeated one-way ANOVA

followed by Tukey test in **F** and a t-test in **G**. *, P<0.05; **, P<0.01. Scale bars equals 60μm in **E** (also for **B**).

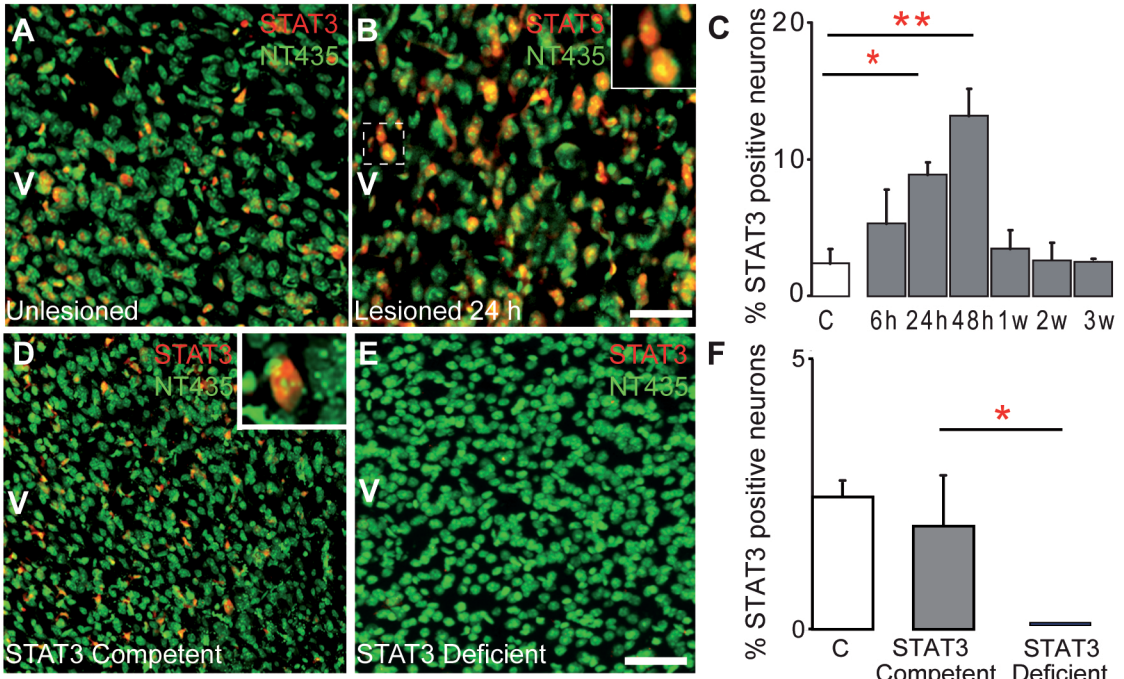

Lang et al., Supplementary Fig. S1

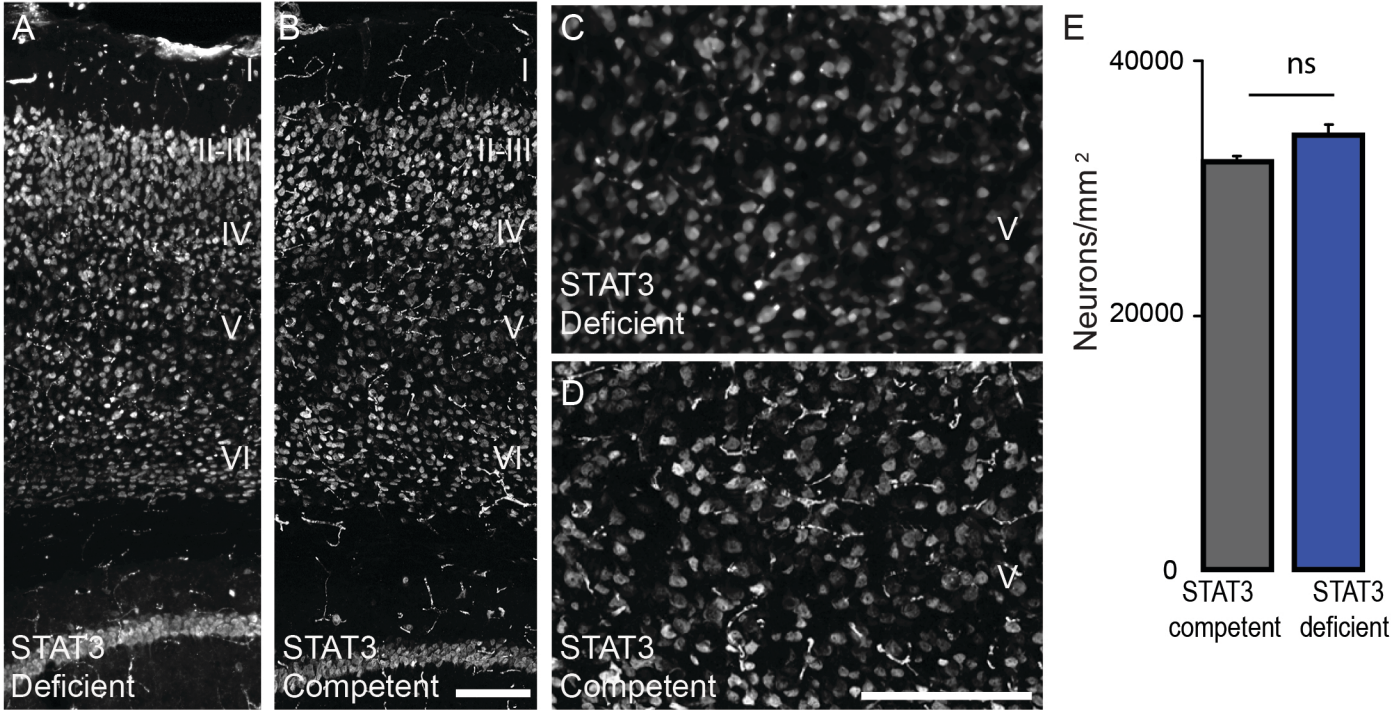

Lang et al., Supplementary Fig. S2

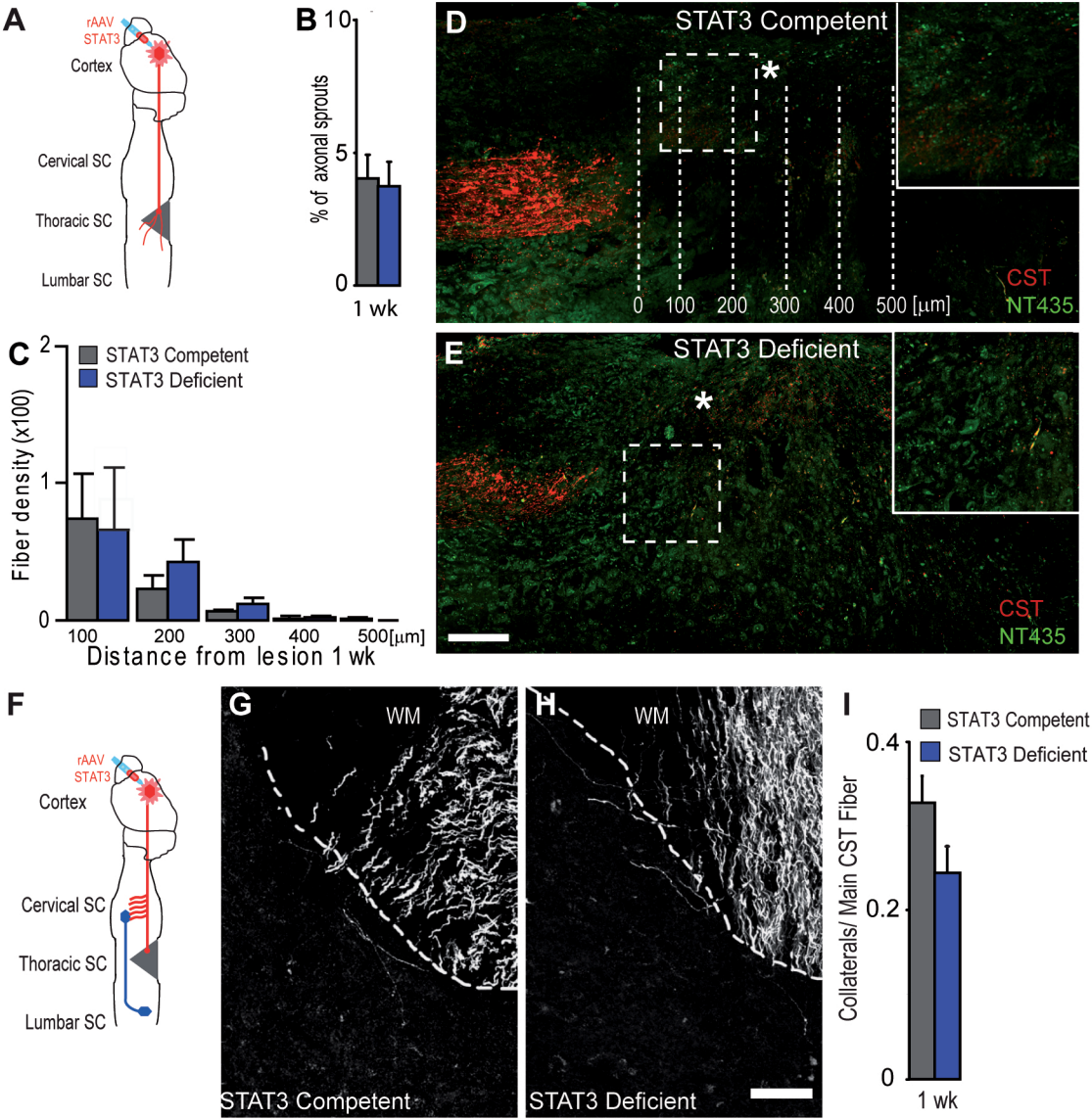

Lang et al., Supplementary Fig. S3

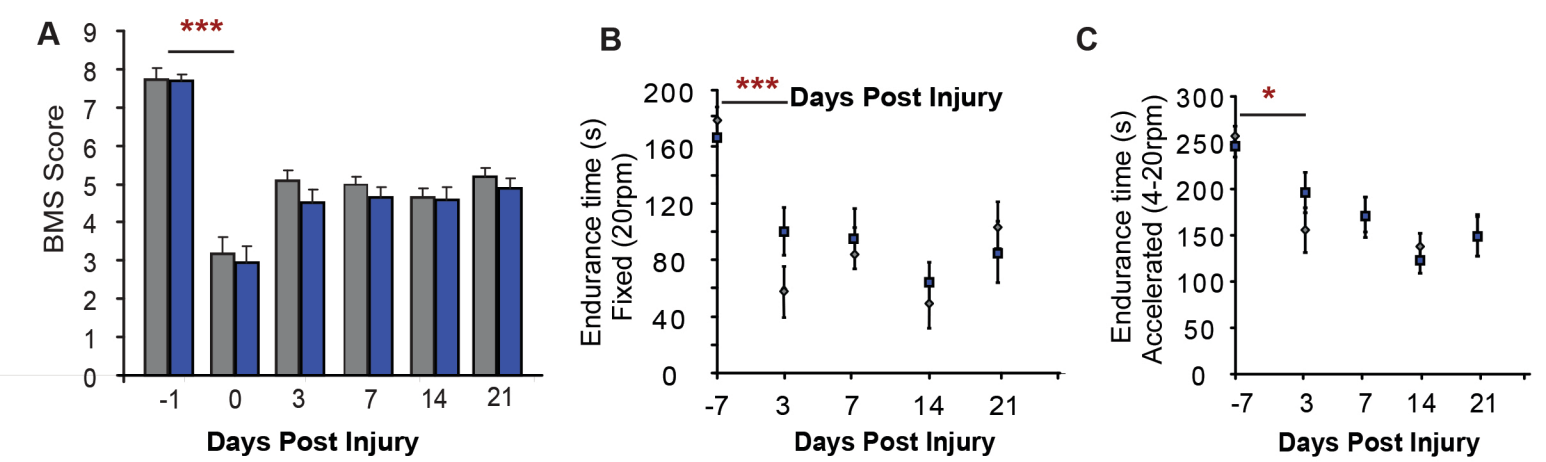

Lang et al., Supplementary Fig. S4

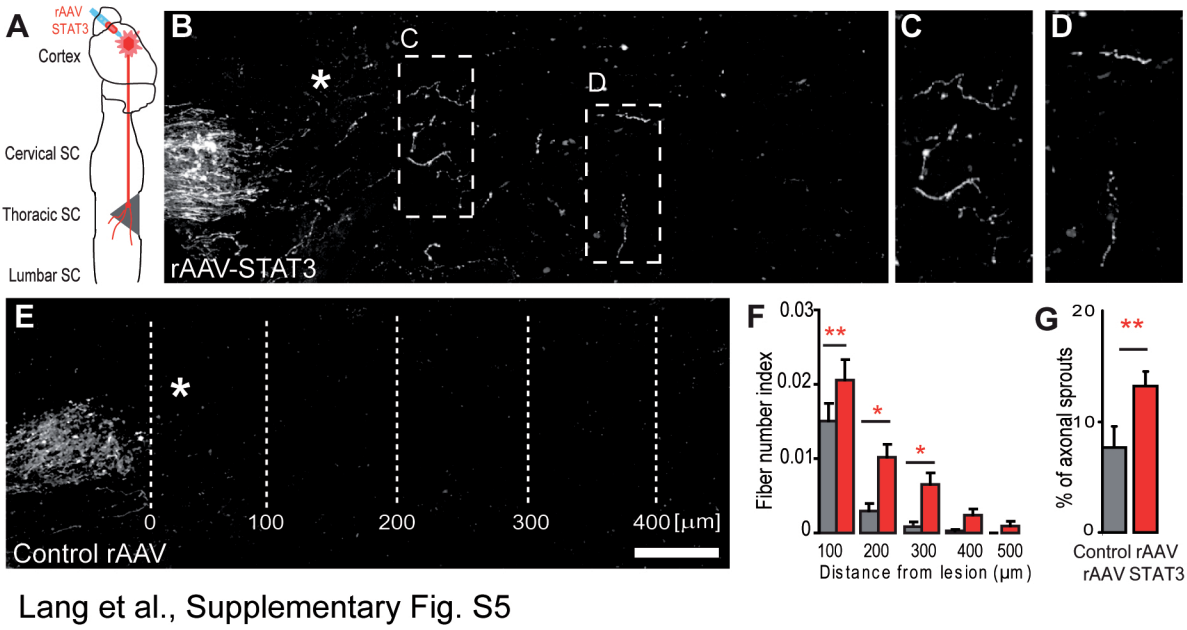

Lang et al., Supplementary Fig. S5